2013 IEEE/RSJ International Conference on
Intelligent Robots and Systems (IROS)
November 3-7, 2013. Tokyo, Japan

InchBot: A novel swarm microrobotic platform

Donghwa Jeong and Kiju Lee

***Abstract*— Collective behavior in swarm robotics explores various scenarios involving many robots communicating, sensing, and running simultaneously. This strategy aims to reduce the time and energy required and to improve the efficiency of completing complex tasks which are typically difficult to accomplish individually. This paper presents *InchBot*, a novel swarm microrobotic platform, which is highly modular, rechargeable, and capable of sensing and communicating with each other wirelessly. InchBot features a new stackable hardware structure allowing customization in the embedded sensors and a novel flexible wheel design suitable for omnidirectional motions. A detailed analysis on the deformation characteristics of the flexible spoke wheels due to centrifugal force was performed using the finite element method. Preliminary experiments demonstrated the utility of flexible spoke wheels for generating forward, diagonal, and turning motions.**

I. Introduction

Swarm robotic platforms have been gaining increasing popularity in the robotics society and have shown a broad range of applications. Such systems have been applied for various purposes from demonstrating/imitating collective behavior found in biological systems, such as social insects including ants, termites, and bees by swarming, flocking, and herding phenomena.

Over the past several decades, many swarm platforms have been developed in different scales with various functionalities [1], [2], [3]. One such platform, Swarm-bots, uses a standard color web cam with a resolution of 640×480 pixels to detect and recognize each other. It uses a gripper based docking mechanism between the robots and communicates through the WiFi module [4]. Kilobot is a small, low-cost platform with vibration-based locomotion and a simple range only sensor using infrared [5]. As another example, e-Puck is equipped with infrared(IR)-proximity sensor, accelerometer, microphone, and camera providing sensory inputs and communicating with the host computer through Bluetooth technology [6]. Due to its variety of available sensors, e-Puck has been used as various robotics research and educational tools [7]. Without using moving parts or mechanisms, an electromagnetic system was also introduced using the electromagnetic coil for locomotion, adhesion, power transfer, communication, and topology sensing [8]. Jasmine is another microrobot consisting of two small DC motors, six IR channels for proximity sensing and communication, and ZigBee communication [9]. I-Swarm is a microrobot ($3 \times 3 \times 3$ [mm^3]) equipped with a solar cell for energy scavenging, optical communication, vibration contact sensor, and piezoelectric legs for locomotion [10].

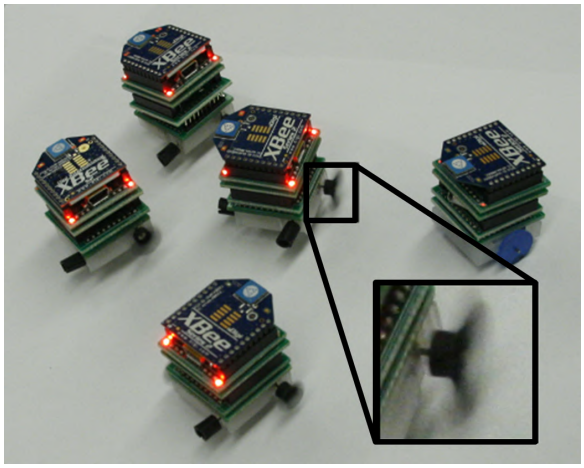

Fig. 1. The InchBot is an 1 inch cube, stackable, agile, and omnidirectional micromobile robotic platform. The omnidirectional locomotion is enabled with flexible spoke wheels.

Despite the attractive features and cost-efficiency, most swarm robots are made with a single body frame that limits hardware extension or modification. Therefore, their functionalities are often limited to the initial specifications. There exists a micromobile robot, called Alice, which can extend its functionality by stacking a communication module and a camera. However, its low performance in the motors, sensors, and power sources constrains its potential applications [12], [13]. The physical size and power are two primary factors that are highly related to the performance and operating time in swarm robotics. One of the most obvious advantages of a smaller robot is its accessibility to narrow places [14]. Small robots can crawl through pipes [15], inspect collapsed buildings [16], or hide in small inconspicuous spaces [17]. For surveillance and exploration tasks, this increased accessibility dramatically impacts the overall functionality of the robots [18]. However, with the small size also comes the disadvantages of limited mobility range, limited energy availability, and possibly reduced sensing, communication, and computation capabilities.

Another challenge in swarm robotics is communication and localization among the robots. Many existing swarm robotic systems use cameras. Camera-based localization can achieve high accuracy, however, the processing can be relatively costly and also its performance is often sensitive to the camera characteristics and external factors [19], [20]. An

Donghwa Jeong is with the Department of Mechanical and Aerospace Engineering, Case Western Reserve University, Email: donghwa.jeong@case.edu

Kiju Lee (Corresponding Author) is with Faculty of Mechanical and Aerospace Engineering, Case Western Reserve University, Cleveland, OH 44106, USA Email: kiju.lee@case.edu

IR-, ultrasound-, or radio-based technique is also commonly used, typically requiring much lower level of processing speed compared to the camera-based one. Ultrasound-based localization, however, requires multiple pairs of emitters and receivers as well as an additional synchronization module that often causes multi-path interferences [21], [22]. IR cameras are less sensitive to external factors, but require line-of-sight for localization. IR proximity sensors usually work within a range of a meter unless an expensive ultra high frequency reader, which can cost more than $500 per module, is used. Radio signal based localization may be realized by two techniques, the time difference of arrival (TDOA) and received signal strength (RSS). TDOA, using radio signals, requires additional hardware implementation to enable high-speed processing. RSS-based techniques are well suited for multirobot applications due to their simplicity, easy identification, communication, and distance sensing capabilities. It still exhibits several technical challenges including data and inconsistent radiation patterns, nonlinearity between RSS data and physical distance values, low signal transmission power which limits the communication range, difficulties in simultaneous mobile localization, and no orientation data. These challenges can be addressed by robust parameter estimation and applying appropriate filtrations to remove outliers [29].

This paper presents a novel stackable swarm microrobotic platform, called InchBot, equipped with a wireless communication module for RSS-based localization and communication. InchBot consists of multiple layers of 1×1 inch^2, 25g stackable boards including a main processor board, a USB programmer and XBee board, an infrared sensor board (optional), a motor driver, an actuator module with wheels, and a power board. Two types of wheels for the chassis boards are developed, one for a typical two-wheel driving system and the other for agile and omnidirectional system using flexible spoke wheels. Although the spoke wheel system has been investigated by several researchers [23], [24], features a unique deformable wheel design using a flexible material that can deform as a wheel by centrifugal force.

II. The InchBot

InchBot is a small mobile robot with limited sensing and communication capabilities. By collaborating with other InchBots as a team or by stacking additional modules on top of the processing board, it can improve its processing, sensing, power, and communication capacities. This section describes the detailed architecture of InchBot.

A. Hardware Architecture

Disadvantages of small-sized robots include limited mobility range, limited energy availability, and possibly reduced sensing, communication and computation ability. Our approach to overcoming these disadvantages is on increased modularity through the stackable board design, novel wheel design, and efficient collaboration among the robots. The

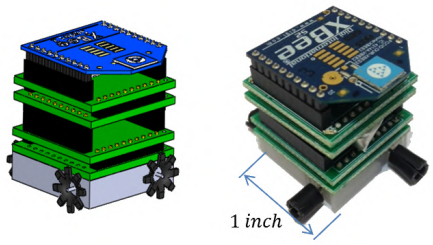

Fig. 2. CAD drawing and physical prototype of InchBot.

primary components of InchBot include actuators, microcontroller, motor driver, batteries, sensors, wireless module, and associated circuitry. Four micro DC motors (6mm in the diameter, typically consumes 120 mA) and two bi-directional motor drivers (LB1836) are the main actuators. The robot is controlled by an ATmega328p microcontroller from ATMEL, which is also characterized by a low power consumption (0.2mA at 1MHz). Small coin batteries were initially considered to power the system, but its low maximal discharging current due to a high internal resistance did not provide enough current for propelling the robot. Therefore, a rechargeable lithium polymer battery (3.7V, 20C, 50mA) was selected.

The system and its functionality can be extended by simply adding additional modules. We adopted the 10×1 pin headers for reliable connections between layers to reduce mechanical failure due to repetitive assembly. Two headers share the common pins so that sixteen digital/analog IO are provided including UART and power. Every module shares the same connector for augmented functionality when stacked together. At the bottom of the motor driver, a different wheel chassis can be attached such as two wheel driving system or four wheel driving system as shown in Fig. 1.

B. Kinematic Model

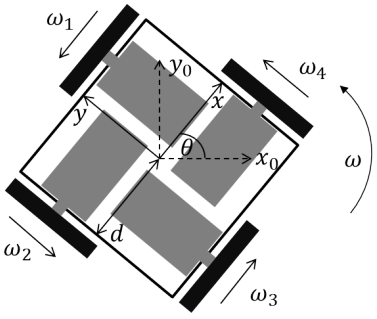

Fig. 3. Four-wheeled robot.

Kinematic model of the following omnidirectional robot at (x, y, θ) shown in Fig. 3 is given by

$$v_y(t) = dy(t)/dt; \quad v_x(t) = dx(t)/dt; \quad \omega(t) = d\theta/dt \qquad (1)$$

The wheel velocity can be obtained by multiplying the deflection of a flexible spoke wheel, δ_n, such as $v_n = \delta_n \cdot \omega_n$

where $n = 1, \cdots, 4$, assuming that the deformation on the wheels at ground contact due to the load is trivial compare to the centrifugal force of the rotating wheels. The relationship between the wheel velocities and robot velocities is:

$$\begin{bmatrix} v_1(t) \\ v_2(t) \\ v_3(t) \\ v_4(t) \end{bmatrix} = \begin{bmatrix} -1 & 0 & d \\ 0 & -1 & d \\ 1 & 0 & d \\ 0 & 1 & d \end{bmatrix} \cdot \begin{bmatrix} v_x(t) \\ v_y(t) \\ \omega(t) \end{bmatrix} \quad (2)$$

From the above equation, the robot speed in relation to the wheel speeds is determined by

$$\begin{aligned} v_x(t) &= \frac{1}{2}(v_3(t) - v_1(t)) \\ v_y(t) &= \frac{1}{2}(v_4(t) - v_2(t)) \\ \omega(t) &= \frac{1}{4d}(v_1(t) + v_2(t) + v_3(t) + v_4(t)) \end{aligned} \quad (3)$$

C. Flexible Spoke Wheel Analysis

When there is no inertial load applied, the flexible spoke wheel is a cylindrical rubber tube as shown in Fig. 4(left). During the locomotion phase, the cylindrical rubber tube is rotated and deformed into a spoke wheel shape by centrifugal force (Fig. 4(right). Due to the nonlinearity of the DC motor between the voltage input and the rotational speed and between the current and the torque in the real world, analyzing a flexible spoke wheel with different shapes/sizes and different number of spokes is challenging without using a well-defined simulation package. To investigate the relationship between the rotational speed and deformation of a flexible spoke wheel, between number of spokes and deformation of flexible spoke wheel, and between the section area where maximum stress is applied and deformation, and further the scaling issues between simulation and actual experimental study, the ANSYS software package with APDL language was used.

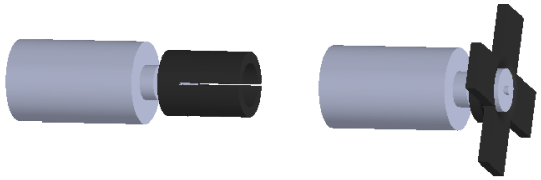

Fig. 4. Flexible spoke wheels when there is no rotational inertial force applied (left) and there exist rotational inertial force causing the four spokes on the cylindrical tubes to be fully extended (right).

1) Centrifugal force and deformation: Centrifugal force applied to the flexible spoke wheel is computed by

$$F = \rho\omega^2 \int_{r_0}^{R} rA(r)dx. \quad (4)$$

where ρ is the density of the flexible spoke wheel, $A(r)$ is the area of section where distance to rotor shaft is r, ω is the rotor's rotational speed (rad/sec), r_0 is the shaft radius, and R is the radius of flexible spoke wheel. The maximum deflection at the tip, δ, and the slope at the free end, θ, can be computed as

$$\delta = \frac{FR^2}{24EI}; \quad \theta = \frac{PR^2}{8EI} \quad (5)$$

where E is modulus of elesticity and I is the moment of inertia of the section.

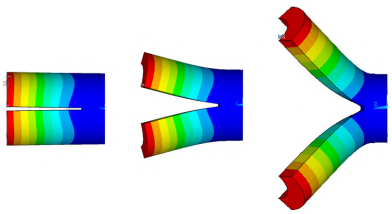

Fig. 5. FEA model for simulating the deformation of the flexible spoke wheel: 0 rad/sec, 100 rad/sec, 200 rad/sec from left to right. Colors are used to indicate the relative amount of deformation by simulation.

2) Nonlinear FEM simulation of deformation: To determine the stress distribution and deflection of the flexible spoke wheel when it is rotated by motors, a model of a cylindrical tube was constructed using FEA for a deformable material, a rigid surface, and inertial loads. The material used for the flexible spoke wheel is polyurethane rubber, an elastomer material with properties of elasticity. The meshed FEA model of the flexible spoke tube is modeled with SOLID 186 which is a 3-D 20-node structural solid [34]. This material has hyper elasticity and the ability to withstand large strains. In addition, each node has three degrees of freedom. The properties applied to the material model are 0.02GPa for Young's modulus, 910 kg/m^3 for the density, and 0.49 for the Poisson's ratio [35]. Fig. 5 shows the FEA deformation model simulated for 0 rad/sec, 100 rad/sec, and 200 rad/sec.

III. Localization and Control Scheme

Localization techniques with wireless communication and distance measuring sensors include 1) received signal strength indication (RSSI) [25], 2) time of arrival (ToA) [26], 3) time difference of arrival (TDoA) [27], and 4) angle of arrival (AoA) [28]. Limited processing capability in such a small robot has shown difficulty in executing the ToA and TDoA methods as theses methods require precise time measurements. Also, AoA requires smart antennas, which are relatively expensive, to measure the angle between the transmitter and receiver node. Although RSSI has a disadvantage that it contains a large amount of outliers and noise, it is easy to implement and requires relatively less complex hardware/algorithms to capture and analyze the received signal strength (RSS). InchBot utilizes the RSSI techniques for communication and localization. The radio signal can not only be used for localization, but may also contain useful information which can be shared among networked robots.

A. Log-distance Path Loss Model

The RSS measurement quantifies the received power of wireless packets sent via the IEEE 802.15.4 protocol. In the real (free space) case, this value varies inversely with the square of the distance and therefore has been suggested as a means to estimate distances between nodes in mobile sensor networks [31], [32]. In order to map the RSS values to the distance measures, we adopt the indoor propagation model based on the log-distance path loss model given by [33]

$$L = L_0 + 10\gamma \log_{10}\left(\frac{D}{D_0}\right) + X_g \tag{6}$$

where L_0 is the pass loss at the distance D_0 measured in decibel (dB), γ is the path loss exponent, and X_g is a Gaussian random variable with zero mean and a standard deviation, σ. Fig. 6 shows the mean RSS values of 10 samples measured at each distance between 2 to 130 [in] where the bar length indicates the standard deviation. The standard deviation tends to increase as the distance becomes greater. Also, the RSS measurements decreases monotonically until about 84 [in] and starts to slow down afterwards. The RSS data was linearly dependent to the $\log_{10}$-distance up to $10^{1.7} \sim 10^{1.8}$, corresponding to $50 \sim 63$ [in]. Therefore, we consider the reliable range of robot-to-robot distance measurements is up to 60 [in], where it follows the $\log_{10}$-distance path loss model in Eq. (6). The estimated parameters for this range are computed by $L_0 = -19.96$ dB, $\gamma = -2.14$, and $d_0 = 2$ [29].

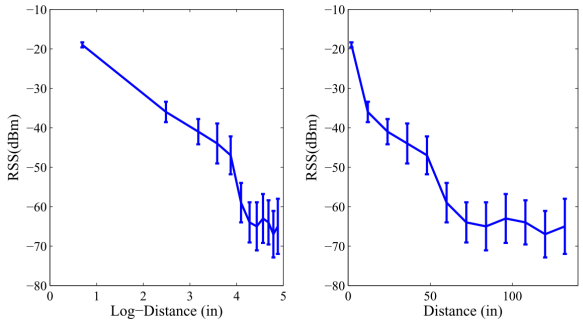

Fig. 6. RSS vs. distance measurements (left) and $\log_{10}$-distance (right) [29].

B. Control Scheme

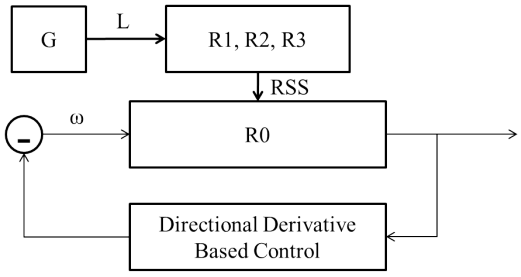

Fig. 7. Schematics of the embedded control method.

The RSS-based cooperative localization technique can be applied for localization of multiple robots. Without using any additional sensor board, such as an infrared sensor, an InchBot with the basic modules (i.e., processor board, XBee communication board, motor driver board, and power board) can locate and track the goal with the directional derivative based control method. The goal (G) and three robots (R1, R2, R3) communicate with each other and determine the position of the goal by received signal strength from the goal as shown in Fig. 7. The goal's location information (L) is then shared with the tracking robot (R0). At the same time, RSS from R1, R2, and R3 coordinates the tracking robot in local coordinates.

Let $\vec{f}^0 = [x_{01}, x_{02}, x_{03}]^T$ be the estimated distance between R0 and three nearest robots based on the RSS. To determine the orientation of G, R0 moves one step, Δx, forward until the RSS value changes. The change in the RSS value informs the robot which direction it should move in local coordinates to reach the goal. The updated distance estimate between R0 and (R1, R2, R3) becomes $(x'_{01}, x'_{02}, x'_{03})$ and the directional derivative of $\vec{f}^0$ with respect to x is given by

$$D_x\vec{f}^0 = \frac{\Delta\vec{f}^0}{\Delta x} = \begin{bmatrix} \frac{x'_{01}-x_{01}}{\Delta x} \\ \frac{x'_{02}-x_{02}}{\Delta x} \\ \frac{x'_{03}-x_{03}}{\Delta x} \end{bmatrix} \tag{7}$$

If the robot is moving toward the goal, the dot product of $D_x\vec{f}^0$ and $\Delta\vec{d}^0$ will be positive where

$$\Delta\vec{d}^0 = \begin{bmatrix} L_{G1} - x'_{01} \\ L_{G2} - x'_{02} \\ L_{G3} - x'_{03} \end{bmatrix} \tag{8}$$

Otherwise, the robot changes its direction by α computed by

$$\alpha = \underset{\theta\in[0,2\pi]}{\arg\max}(D_x\vec{f}^0 \cdot \Delta\vec{d}^0) \tag{9}$$

Fig. 8 illustrates the described control scheme for locating a single goal.

IV. Preliminary Experiments

Our preliminary experiments focused on testing the utility of flexible spoke wheels for generating forward, diagonal, and turning motions. Detailed description on RSS-based communication techniques that can be implemented in InchBots can be found in [29].

A. Agility in proposed locomotion

The flexible spoke wheels are not perfectly uniform due to manufacturing errors. Therefore, it requires a calibration process by giving the robot weight factors to each wheel to move the same distance. The InchBot is slippery on the ground but highly agile (faster than 450mm/sec) as shown in Fig. 9.

To evalaute the robot's speed for different duty cycles, 100% duty cycle (3.3V), 75% duty cycle (2.475V), and 50% duty cycle (1.65V) of PWM inputs were tested. Fig. 9 shows that the robot moves with increasing speed. Also, high speed

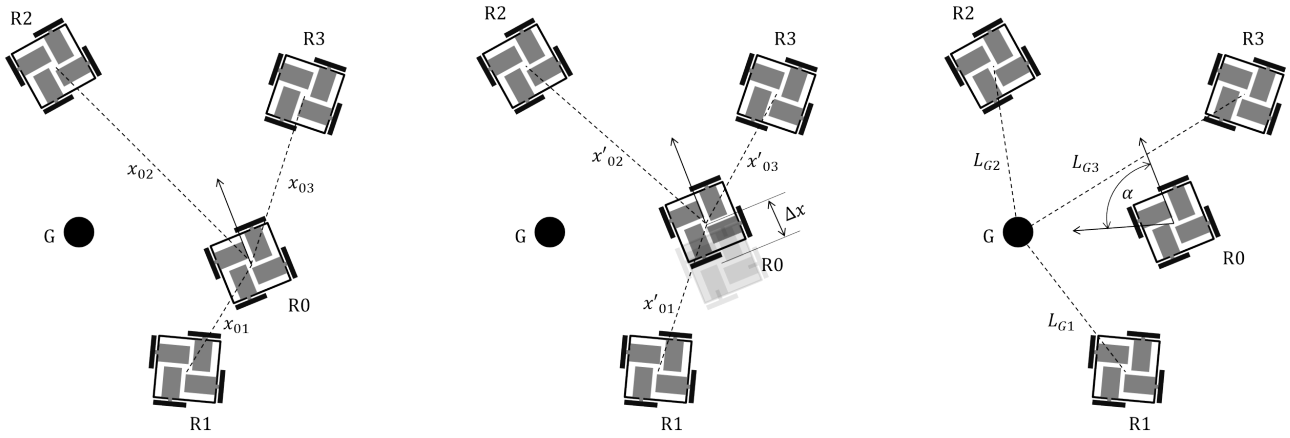

Fig. 8. Illustration of directional derivative-based control scheme; R0 is moving robot, R1, R2, and R3 are reference robot, and G is goal. R0 moves one step and receives signal strength from R1, R2, R3, and G to estimate the position and change the direction.

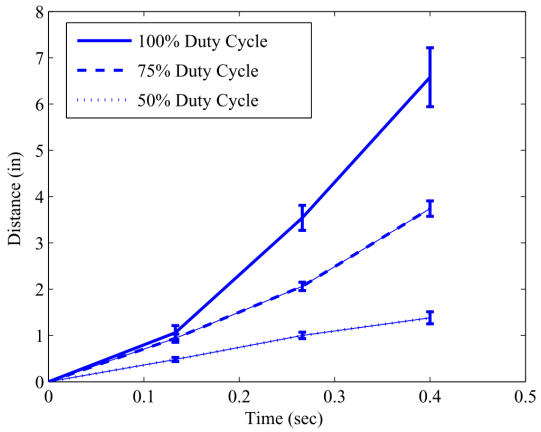

Fig. 9. Distance versus time for three different duty cycles. Five trials are performed for each duty cycle.

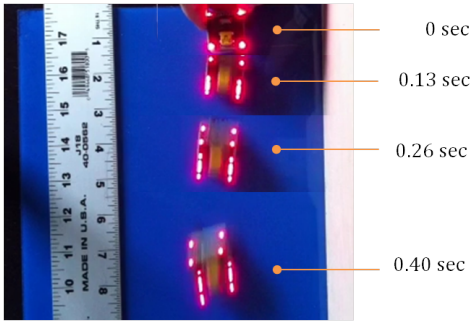

Fig. 10. Forward motion experiment (the video is attached to this paper).

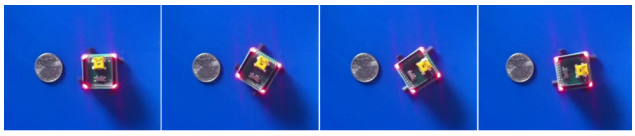

Fig. 11. Turning motion experiment (the video is attached to this paper).

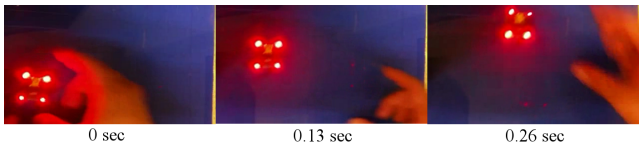

Fig. 12. Diagonal motion experiment (the video is attached to this paper).

motion has more slip when it starts moving whereas low speed motion has less initial slip. The robots were placed on an acrylic plate and recorded with an overhead camera so that distance and time could be retrieved with collected video files.

B. Forward, Diagonal, and Turning motions

The proposed locomotion allows the consideration of much simplier robot control. Without steering the wheels, the InchBot is capable of omnidirectional locomotion. To demonstrate the locomotion, forward, diagonal, and turning motions were tested by changing the speed of rotation of each flexible spoke wheel. Fig. 10 shows a forward motion by rotating two motors. As shown in Fig. 9 and Fig. 10, robot accelerates due to the slip between the wheel and the ground during high speed motion. Some of the challenges, such as consistent speed control, remains as future work. Different material selection for the wheel could be a possible solution for this. Fig. 11 and 12 show turning motion by rotating a single motor and diagonal motion by using two motors.

V. Conclusion and Discussion

This paper presented a novel swarm microrobotic platform, InchBot, with highly modularized and expandable features. To validate the functionality of flexible spoke wheels, finite element analysis and preliminary experiments were conducted for analyzing the deformation characteristics and demonstrating forward and turning motions. The robots can be fully equipped to utilize RSS-based techniques, such as the algorithms we presented in [29]. InchBot is one of the

smallest swarm microrobotic platform with improved communication capabilities and expandable/adaptable features that make InchBot uniquely positioned among the others. Regarding the size, a single robot can typically offer better performace when it is large whereas the tiny robot is limited in its functionality. As the swarm robots pursue small size, IR sensors are equipped in all robots except for the I-Swarm (I-Swarm is too small to embed IR). InchBot also features its speciality in omnidirectional locomotion and low cost (less than $50 components in cost including the XBee wireless module).

The flexible spoke wheels successfully demonstrated omnidirectional motion, by moving forward (either in an x or y direction) and diagonally, and turning at the same position. However, precise trajectory and speed control of the InchBot with spoke wheels is still a challenging technical issue. We are currently working on improving our ANSYS simulation, including the surface model and conducting experiments to determine control parameters and reduce uncertainty.

ACKNOWLEDGEMENT

This work was partially supported by the National Science Foundation under Grant No. 110927.

REFERENCES

[1] A. Gutierrez, A. Campo, M. Dorigo, J. Donate, F. Monasterio-Huelin, and L. Magdalena, "Open E-puck Range & Bearing Miniaturized Board for Local Communication in Swarm Robotics," *IEEE International Conference on Robotics and Automation*, pp. 3111 - 3116, 2009.

[2] J. Haverinen, M. Parpala, and J. Roning, "A Miniature Mobile Robot With a Color Stereo Camera System for Swarm Robotics Research," *IEEE International Conference on Robotics and Automation*," pp. 2483-2486, 2005.

[3] S. Kornienko, O. Kornienko, and P. Levi, "Minimalistic approach towards communication and perception in microrobotic swarms," *IEEE/RSJ International Conference on Intelligent Robots and Systems*, pp. 2228 - 2234, 2005.

[4] F. Mondada, G. C. Pettinaro, A. Guignard, I. V. Kwee, D. Floreano, J. L. Deneubourg, S. Nol, L. M. Gambardella, and M. Dorigo, "SWARM-BOT: A New distributed robotic concept," *Autonomous Robots*, 17(2/3):19322, 2004.

[5] M. Rubenstein, C. Ahler, and R. Nagpal, "Kilobot: A Low Cost Scalable Robot System for Collective Behaviors," *IEEE International Conference on Robotics and Automation*, pp.3293-3298, 2012.

[6] F. Mondada, M. Bonani, X. Raemy, J. Pugh, C. Cianci, A. Klaptocz, S. Magnenat, J. C. Zufferey, D. Floreano, and A. Martinoli, "The e-puck, a Robot Designed for Education in Engineering," *Proceedings of the 9th Conference on Autonomous Robot Systems and Competitions*, 1(1) pp. 59-65, 2009.

[7] H. Guo, Y. Meng, and Y. Jin, "Swarm Robot Pattern Formation using a Morphogenetic MultiCellular based Self-organizing Algorithm," *IEEE International Conference on Robotics and Automation*, 2011.

[8] B. Kirby, B. Aksak, J. Hoburg, T. Mowry, P. Pillai, "A Modular Robotic System Using Magnetic Force Effectors," *IEEE International Conference on Intelligent Robots and Systems*, pp. 2787-2793, 2007.

[9] S. Kernbach and O. Kernbach, "Collective energy homeostasis in a large-scale microrobotic swarm," *Robotics and Autonomous Systems*, 2011.

[10] P. Corradi, T. Schmickl, O. Scholz, A. Menciassi, and P. Dario, "Optical Networking in a Swarm of Microrobots," *In Proc. Third International Conference on Nano-Networks (Nano-Net 2008)*, Boston, 2008.

[11] J. Pugh, X. Raemy, C. Favre, R. Falconi, and A. Martinoli, "A fast onboard relative positioning module for multirobot systems," *IEEE/ASME Transactions on Mechatronics*, vol. 14, no. 2, pp. 151-162, 2009.

[12] G. Caprari, R. Seigward, "Mobile Micro-Robots Ready to Use: Alice," *IEEE/RSJ International Conference on Intelligent Robots and Systems*, 2005.

[13] G. Caprari, T. Estier, R. Siegwart, "Fascination of Down Scaling - Alice the Sugar Cube Robot," *Journal of Micro-Mechatronics*, Vol. 1, pp. 177 - 189, 2002.

[14] L. E. Navarro-Serment, R. Grabowski, C. J. J. Paredis, P. K. Khosla, "Modularity in small distributed robots," *In Proceedings of the SPIE conference on Sensor Fusion and Decentralized Control in Robotic Systems II*, 1999.

[15] S. Wakimoto, J. Nakajima, M. Takata, T. Kanda and K. Suzumori, "A Micro Snake-like Robot for Small Pipe Inspection," *Proceedings of International Symposium on Micromechatronics and Human Science*, pp. 303 - 308, 2003.

[16] H. Schempf, "Self-rappelling Robot System for Inspection and Reconnaissance in Search and Rescue Applications," *Advanced Robotics*, pp. 1 - 30, 2009.

[17] R. Grabowski, L. E. Navarro-Serment, C. J. J. Paredis, P. K. Khosla, "Heterogeneous Teams of Modular Robots for Mapping and Exploration," *Journal Autonomous Robots*, Vol. 8, Iss. 3, pp. 293 - 308, 2000.

[18] J. McLurkin and J. Smith, "Distributed Algorithms for Dispersion in Indoor Environments Using a Swarm of Autonomous Mobile Robots," *Distributed Autonomous Robotic Systems*, Vol. 6, pp. 399 - 408, 2007.

[19] S. Se, D. Lowe, J. Little, "Vision-based mobile robot localization and mapping using scaleinvariant features," *IEEE International Conference on Robotics and Automation*, 2001

[20] P. Blaer, P. Allen, "Topological Mobile Robot Localization Using Fast Vision Techniques," *IEEE International Conference on Robotics and Automation*, 2002.

[21] H. Lin , C. Tsai, J. Hsu, C. Chang, "Ultrasonic self-localization and pose tracking of an autonomous mobile robot via fuzzy adaptive extended information ltering," *IEEE International Conference on Robotics and Automation*, 2003.

[22] N. B. Priyantha, A. Chakraborty, and H. Balakrishnan, "The Cricket Location-Support System, *Intl Conf. on Mobile computing & networking*, 2000.

[23] P. Tantichattanont, S. Songschon, and S. Laksanacharoen, "Quasi-Static Analysis of a Leg-Wheel Hybrid Vehicle for Enhancing Stair Climbing Ability," *IEEE International Conference on Robotics and Biomimetics*, pp. 1601 - 1605, 2008.

[24] B. G. A. Lambrecht, A. D. Horchler, and R. D. Quinn, "A Small, Insect-Inspired Robot that Runs and Jumps," *IEEE International Conference on Robotics and Automation*, pp. 1240 - 1245, 2005.

[25] M. Sugano, T. Kawazoe, Y. Ohta, and M. Murata, " Indoor Localization System using RSSI Measurement of Wireless Sensor Network based on ZigBee ," *Proceeding of Wireless Sensor Networks*, 2006.

[26] Q. H. Spencer, B. D. Jeffs, M. A. Jensen, and A. L. Swindlehurst, "Modeling the Statistical Time and Angle of Arrival Characteristics of an Indoor Multipath Channel," *IEEE Journal of Selected Areas in Communications*, Vol. 18, No. 3, pp. 347 - 360, 2000.

[27] F. Gustafsson and F. Gunnarsson, "Positioning using Time-difference of Arrival Measurements," *IEEE International Conference on Acoustics, Speech, and Signal Processing*, Vol. 6, pp. 553 - 556, 2003.

[28] A. Abdi, J. A. Barger, M. Kaveh, "A parametric model for the distribution of the angle of arrival and the associated correlation function and power spectrum at the mobile station," *IEEE Transactions on Vehicular Technology*, Vol. 51, Iss. 3, pp. 425 - 434, 2002.

[29] D. Jeong and K. Lee, "Directional RSS-Based Localization of Multi-Robot Applications," *12th WSEAS International Conference on Signal Processing, Robotics, and Automation*, Cambridge, UK, February 2013.

[30] R. Michaelis, R. Mutti, J. Overmyer, O. Taylor, "All About Motors an NJATC Textbook," *Thomson*, pp. 202-211, 2004.

[31] C. Perkins et al., "Distance sensing for mini-robots: RSSI vs. TDOA," *IEEE International Symp. on Circuits and Systems (ISCAS)*, 2011.

[32] J. Hill, R. Szewczyk, A. Woo, S. Hollar, D. Culler, and K. Pister, "System architecture directions for networked sensors," *ACM SIGPLAN Notices*, vol. 35, no. 11, pp. 93-104, 2000.

[33] J. S. Seybold, "Introduction to RF Propagation," *Wiley Interscience*, September 2005.

[34] Release 11.0 Documentation for ANSYS, ANSYS Inc., 2007.

[35] Science Data Book, Edited by R. M. Tennent, Oliver & Boyd, 1976.